Cohesion and agglomeration of wet powders

Pascal S. Raux and Anne-Laure Biance*
Institut Lumière Matière, UMR5306 Université Lyon, 1-CNRS Université de Lyon, 69622 Villeurbanne, France

(Received 21 November 2016; published 29 January 2018)

Wet high-shear granulation consists in vigorously mixing grains and a liquid binder to create agglomerates of various sizes. The process results from a balance between cohesion of the wet granular agglomerates and fragmentation due to the high mixing. By performing a simple test with glass beads and various liquids, we first focus on the static cohesion of wet granular media. Contrary to previous works, we extend the study to larger values of the liquid fraction w. After the well-documented plateau, the cohesive strength increases again with w, a behavior we capture by a simple model. We then focus on the dynamical cohesion of the media and we design an agglomeration process that consists in vibrating a bead/liquid mixture at a large amplitude. The vibrations induce not only the fluidization of the wet granular material but also the formation of aggregates. As expected, their size is affected by the liquid content, the frequency, and the amplitude of the vibrations, similarly to high-shear granulation data. However, the number of beads in an agglomerate does not depend on the bead size, showing a self-similar mechanism of agglomeration. The role of the static cohesion strength in this dynamical process remains therefore ambiguous.

DOI: 10.1103/PhysRevFluids.3.014301

I. INTRODUCTION

Granulation refers to a process that consists in assembling fine dispersed particles to create larger ones, called agglomerates or granulates. Achieved everyday in all the industry sectors involving powders (pharmaceutical, building, cosmetics, food, detergency, etc.), this transformation aims essentially at storing, mixing, or handling the powder. Depending on the desired applications, different strategies have been defined for the granulation process, including pressing in a dry environment or adding a chemical or physical binder to induce cohesion. When only liquid is added to create capillary-based cohesion between the powder grains, the process is called wet granulation [1]. A very common way to granulate in a wet environment is the so-called *high-shear granulation* process [2], which consists in rotating impellers with complex geometry at high velocity and in large tanks. The success of this process is empirical and depends on the type of powder used, the impeller geometry, the rotation rate, the tank size, and the nature or amount of the added binder. More fundamentally, granulation belongs to the class of agglomeration mechanisms encountered in many situations such as ash gas during volcanic eruptions [3], star formation [4], or biological tissue fabrication [5]. The agglomerate formation results from a balance between fragmentation and aggregation processes, which needs to be identified to describe thoroughly the mechanical factors affecting the size of the resulting agglomerates.

We draw here a physical picture of high-shear granulation in two steps with two model experimental systems. First, we propose a static test of cohesion in well-controlled wet granular media on a large range of binder fraction w, defined as the ratio of the liquid volume over the solid volume. The range of w is chosen to match the experimental conditions of high-shear granulation

*anne-laure.biance@univ-lyon1.fr

[2]. By analyzing the liquid repartition within the grains, we capture our results with a simple modeling. Second, we propose an experimental procedure to test the dynamical cohesion of the media and to control the agglomeration process. We then show that this simple procedure bears the same characteristics of a high-shear granulator.

II. STATIC: COHESIVE STRENGTH

The static cohesion of an assembly of wet grains has been widely studied both theoretically and experimentally [6–9]. The first works attempted to determine the capillary force between two grains [6–8], taking into account the liquid volume, the surface roughness [6], or the solid elasticity [9,10]. Subsequent challenges have been to show the impact of this local nonlinear force to a random assembly of grains linked by liquid bridges[11–14]. Different experimental techniques have been developed to measure the internal stress of wet granular media, such as the draining crater experiment [7], the critical angle of response determination [15], or the maximal centrifugation sustained before rupture [12]. However, most of the work is devoted to a low liquid fraction ($w < 5\%$–10% with our notations), in the vicinity of the so-called pendular regime, where isolated liquid bridges ensure the stability of the wetted granular media [16]. At a higher liquid content, the structure of the liquid repartition switches from the pendular regime to the funicular one where liquid bridges are connected. For $2\% \leqslant w \leqslant 25\%$, a saturation (plateau) of the rupture stress with the liquid content is observed [12,17,18]. From a theoretical point of view, the cohesion force induced by complex liquid repartitions has been recently studied, such as the merging of three meniscii leading to trimers [19]. They show that the saturation should stand. However, the observation of a subsequent increase at a larger liquid fraction in engineering tests [16,20,21] remains mostly undocumented.

A. Experimental methods

We conducted experiments using a model granular material consisting of spherical borosilicate beads (Sigmund-Lindner) of density $\rho_s = 2500$ kg/m^3. The beads are thoroughly cleaned with soap (decon) and de-ionized water and placed in an ultrasonic bath before the experiments. The beads are sieved and five samples with different mean diameters d are used: 52 ± 8, 71 ± 10, 105 ± 7, 146 ± 19, and 207 ± 22 μm. The typical roughness of the beads measured by atomic force microscopy (AFM) is 10 nm (peak to peak). Given the range of liquid content studied ($w > 1\%$), it should not influence the cohesive stress [6]. The beads are then gently stirred by hand with the binding liquid for approximately 1 min, until a homogeneous paste is obtained. The details of the mixing protocol and the mixing time do not affect the results as long as evaporation is prevented. We then compact the wet beads between two parallel plates in three directions repeatedly with a typical pressure of a few bars. A razor blade is used to remove the excess beads and form a parallelepipedic beam of width W and thickness H. We measure the solid fraction ϕ by weighing the beam before and after drying it, and present the results in Fig. 1(a). The value of ϕ is lower than the one of the dry grains: Cohesive granular materials are known to have a lower density than dry ones. Leaving apart the dry case, we observe a slight increase in the solid fraction with the liquid content. Such densification with the liquid content w is commonly observed for soil and industrial powders [22]. In our range of w, we approximate this weak trend by a linear law $\phi(w)$ [Fig. 1(a)].

We use the beam weight to apply a stress inside the material: The beam is pushed at a typical speed of 1 mm/s towards an edge until it breaks at a critical length L [Fig. 1(b), inset]. Several beam sizes are tested for each granular material composition. Figure 1(b) presents results obtained for a given grain size, at a given liquid content. L does not vary with W (tuned by a factor 5) but increases with the thickness, scaling as $\sqrt{H}$.

B. Experimental results

A wet granular medium is a cohesive material, and we model its mechanical behavior only with a mean cohesive stress σ beyond which the material breaks. As the free-standing length increases,

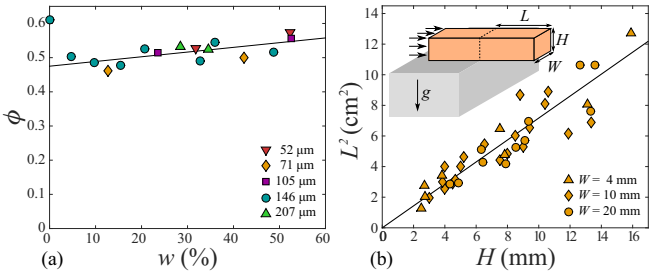

FIG. 1. (a) Solid volumic fraction vs liquid content, for different grain diameters. (The binding liquid is water.) The line shows the linear fit $\phi \approx 0.47 + 0.13w$. (b) Square of the rupture length as a function of the beam thickness, for various widths. Here, $d = 71$ μm and $w = 25\%$. The line gives the best fit, of slope 72 mm. Inset (experiment principle): The granular beam breaks under its own weight at an overhanging length L.

the internal stresses inside the beam build up: Gravity applies a torque on the free-standing part of the beam, scaling as $\rho g H W L^2$. Rupture of the beam occurs when this torque exceeds the cohesive strength σ, whose torque scales as $\sigma W H^2$. Thus, the balance of torques reduces to

$$L^2 = \frac{\sigma}{\rho g} H. \tag{1}$$

As $\sigma/\rho g$ does not depend on the geometry of the beam but only on the material properties, this expression captures well the experimental data presented in Fig. 1. We can specify the relationship between L^2 and H by developing the expression of $\rho = \phi(\rho_s + \rho_l w)$, where ρ_l is the liquid density. All the quantities are constant, except ϕ and the liquid content w, measured in each experiment. The cohesive strength σ is then determined through the slope of the linear relationship between L^2 and H,

$$\sigma = \phi g(\rho_s + \rho_l w)\frac{L^2}{H}. \tag{2}$$

Figure 2 presents the normalized cohesive strength σ measured from beam rupture experiments using Eq. (2) for various grain diameters and liquid content w. Two regimes are observed: a plateau and then an increase of the strength as a function of w.

The expression of the force F of a single capillary bridge has two contributions [8,23]. One is due to the difference of pressure ΔP in the curved meniscus $F_p = -\Delta P \pi d^2 \sin^2(\psi)/4$, and the other due to the surface tension at the solid/liquid contact line $F_s = \pi d\gamma \sin(\psi)\sin(\psi + \theta)$, with ψ corresponding to the filling angle [23], related to w, and θ the liquid/bead contact angle, close to zero here.

At low w, the two contributions compensate and the force reduces to $F \simeq \pi d\gamma \cos\theta$, independent on the volume of the liquid bridge: The cohesion is constant (horizontal line) as a function of w, as expected in the pendular and early funicular regime [12]. Assuming that Z independent capillary bridges are contributing to cohesion on average for each grain, we derive from the previous expression the mean macroscopic stress,

$$\sigma = 4Z\epsilon_s \frac{\gamma \cos\theta}{d}, \tag{3}$$

where ϵ_s is the surface solid fraction in a section of the granular material and $\theta \approx 0$ for wetting liquids. According to Eq. (3), the cohesive strength scales as γ/d, which is well captured in our experiments, as the data from all bead samples collapse on a single master curve. We also varied the liquid binder, using water ($\gamma = 73$ mN/m and viscosity $\eta = 1$ mPa s), glycerol ($\gamma = 63$ mN/m, $\eta = 990$ mPa s), and silicon oil ($\gamma = 22$ mN/m and $\eta = 20$ mPa s). As shown in the inset of Fig. 2, no effect of the viscosity is found and the effect of surface tension is also rationalized by expression

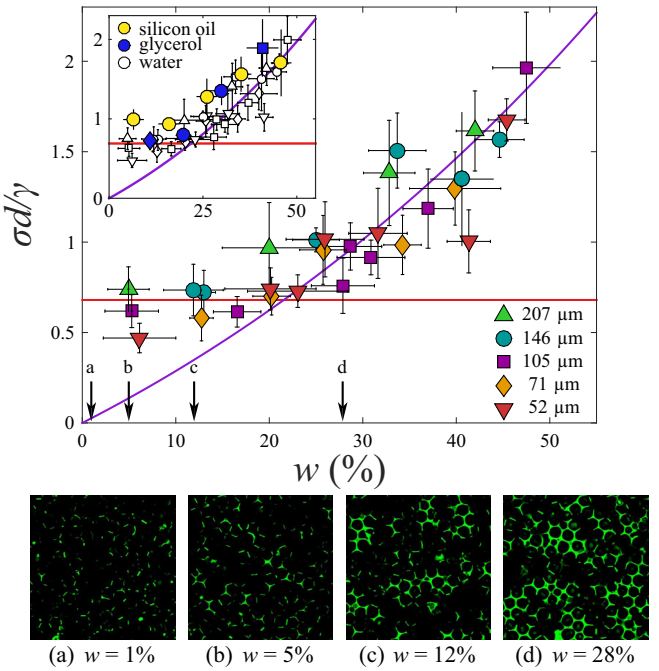

FIG. 2. Normalized cohesive stress as a function of the liquid content (here, water) for various grain sizes. Each value of σ is derived from at least eight measurements of critical length L against thickness H and using Eq. (2). The two regimes discussed in the text are shown with colored lines: $\sigma d/\gamma \approx 0.7$ in red and Eq. (7) in purple, with $K = 6.4$. Inset: Same measurements, obtained for different liquids. (a)–(d) Examples of images taken with confocal microscopy. For these images, we used glycerol with fluorescein and $d = 71$ μm. The width of each image corresponds to 920 μm.

(3). A slight shift is observed, which can be attributed to several factors, such as nonzero contact angles, dust, or other contaminations of the liquids.

This regime of constant cohesion extends in the funicular regime ($w > 5\%$), well beyond the limit at which the capillary bridges start to merge. Scheel *et al.* measured the cohesive strength of wet glass beads by centrifugation [12] and reported a constant stress $\sigma = 220$ Pa in the domain $1\% < w < 26\%$, so well beyond the pendular regime. Approaching their surface tension with the one of water, it corresponds to $\sigma d/\gamma \approx 0.9$, similar to the approximately constant cohesive stress obtained here at low w around $0.7\gamma/d$ in the same range. Koos *et al.* [24] also measured in a rheometer the yield stress of a suspension to which a secondary fluid is added (hematite of 5 μm in diisononyl phthalate (DINP) with a small amount of water), reporting a maximum versus water volume fraction of 2000 Pa. Assuming that their liquid/liquid surface tension is around 10 mN/m, the obtained value remains in good agreement with our measurement, showing the robustness of the value of the plateau with different systems.

However, here, at a larger liquid content, a different phenomenon, an increase of cohesion, is observed for $w > 20\%$ (Fig. 2). To apprehend this result, we inspect the liquid repartition in the granular material using fluorescence confocal microscopy (Leica TCS SP5DMI6000, objective $\times 10$, numerical aperture NA $= 0.3$). To prevent evaporation during the recording, fluorescein-loaded glycerol is used as the binding liquid. Due to the difference in the refractive index between glass and air, no visualization was possible deep inside the granular material: Only the first two layers of grains are then observed, preventing quantitative measurements. Figure 2 shows the pictures reporting an evolution of the liquid repartition: At low w, isolated capillary bridges in the pendular regime are observed [Fig. 2(a)]. They start to connect to each other at higher w [Fig. 2(b)], forming small liquid

clusters (funicular regime). The clusters grow and progressively invade all the voids between the grains [Figs. 2(c) and 2(d)] as w increases. Note that the bridges connect at a relatively low water content w: Our experiments are thus mainly in the cluster (funicular) regime. Moreover, in the domain showing an increase of the cohesive strength, a unique cluster is expected to regroup all of the liquid [12].

C. Discussion

To understand these two behaviors (the plateau and the subsequent increase), one must first note that in these ranges of w, the two contributions of the force of the capillary bridges no longer compensate. The pressure contribution F_p indeed overcomes the surface tension one, F_s. The mean cohesive strength σ can then be estimated from the average pressure exerted by the liquid on the grain assembly. Following the two-dimensional (2D) numerical analysis of Ref. [13], σ is thus related to the liquid capillary pressure p_l, the packing fraction ϕ, and the ratio of the wetted grain surface S_{wet} over the total grain surface S_{sol},

$$\sigma = p_l \phi \frac{S_{\text{wet}}}{S_{\text{sol}}}. \tag{4}$$

To quantify σ, one needs to evaluate both the pressure inside the liquid phase and the grain wetted surface. For an isolated liquid bridge, the pressure p_l is defined by a geometrical relationship and is shown to decrease (in absolute value) as the bridge volume increases. When the funicular regime is reached (i.e., when the capillary bridges merge to form clusters), Scheel *et al.* [12] showed by x-ray tomographic measurements that the pressure saturates to a value of $-K\gamma/d$ with a constant $K \approx 9$. Similar results were obtained for trimers by a numerical analysis [19]. As most of the clusters connect, we assume here that we can extend this result to the full range of liquid content studied ($4\% < w < 50\%$).

We now consider the variations of the grain wetted surface with w. In small liquid clusters (just after the merging), it remains almost constant, as the added liquid fills the gap between the grains without affecting the wetted surface. For example, in an ideal compact packing, filling tetrahedral and octahedral spherical cavities with liquid is not associated with any increase of the wetted surface, while it requires an increase of w by 9%. A similar phenomenon is expected in the densest regions of the granular material. Thus, in the early funicular regime, S_{wet} does not depend on the liquid content and Eq. (4) leads to a constant cohesive strength, as observed. On the contrary, inside larger clusters, most of the pores are already saturated by the liquid [see Fig. 2(d)]. In this limit of large w, the wetted area can be approximated by the total surface of the grains in the cluster, i.e., πd^2 for each grain, while the liquid volume is close to the available pore space, related to the total volume of grains V_s and ϕ [25]. The ratio of the wetted area of the grains to the liquid volume V_l for a cluster filled with liquid thus reads

$$\frac{S_{\text{wet}}}{V_l} \approx \frac{6\phi}{d(1-\phi)}, \tag{5}$$

while the geometrical relationship for spherical grains leads to $S_{\text{sol}} = 6V_s/d$. Assuming that Eq. (5) is representative of the surface/volume relationship in our clusters, one can thus rewrite Eq. (4), using $w = V_l/V_s$,

$$\sigma = p_l \frac{\phi^2 w}{1-\phi}. \tag{6}$$

Following the results of Refs. [12,19], we deduce the cohesive strength in the limit of large clusters,

$$\sigma = \frac{K\gamma}{d} \frac{\phi^2 w}{1-\phi}. \tag{7}$$

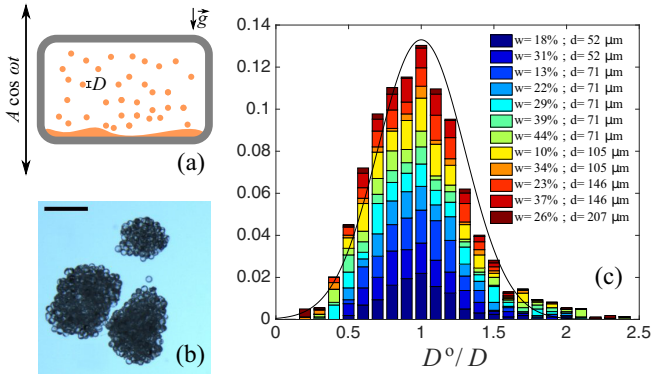

FIG. 3. (a) When wet granular material is vibrated in a box, and agglomerates are formed, with a mean size D. (b) Picture of agglomerates obtained from $d = 146$ μm grains with $w = 37\%$ and $A\omega = 0.9$ m/s. Scale bar: 1 mm. (c) Normalized size distribution for various grain sizes d and water content w, showing a common distribution even though the mean agglomerate size D varies. Gaussian distribution is displayed to show the slight asymmetry in this distribution.

For a constant ϕ, we thus expect a linear relationship between the normalized cohesive stress and w, with a coefficient that is $K\phi^2/(1-\phi)$. Using Eq. (7) and the linear fit from Fig. 1(a), the curve in Fig. 2 shows that this equation describes correctly our measurements of σ. As we defined the cohesive stress in the two regimes [Eqs. (3) and (7)], the liquid fraction at the transition $w \simeq 4Z\epsilon_S(1-\phi)/(K\phi^2)$ is around 20%, in agreement with our experiments. Using Eq. (4), we also estimate that, in the plateau regime, 15%–20% of the surface of the grains is wetted by the liquid. On average, one grain is then surrounded only by two or three connected large capillary bridges. This shows that the liquid is inhomogeneously repartitioned, in good agreement with the images of Fig. 2.

We then designed a simple experimental test to determine the cohesion stress of wet granular media in a static condition in a large range of liquid fraction. On the one hand, at a low liquid content (for $w < 20\%$), the grain wetted area and the liquid pressure do not vary, which explains the well-documented plateau. On the other hand, at a larger liquid content, an increase of the stress attributed to the increase of the wetted area is observed. These results, captured by a simple scaling, agree qualitatively well with some low documented engineering data [16,20]. One can notice that this model depends strongly on the liquid repartition and its inhomogeneity. Different protocols of sample preparation could lead to different capillary pressure dependencies, as shown in recent numerical simulations [13]. Moreover, the effects of polydispersity and angularity of the grains can also explain the equivocal comparison with more realistic granular materials [26].

III. DYNAMICS: GRANULATION

A. Experiments

Now that the cohesive strength of wet granular media is well described, we investigate it under dynamical conditions and, in particular, in the context of high-shear granulation. By a closer look, most of the process stands in the impact of the agglomerates with the impellers [27]. We therefore switch to a more controlled setup by using a large amplitude vibrating pot to agglomerate our beads (Fig. 3). The vibration of dry grains has been largely studied [28–31] as it is used as a way of compacting the material. From a more physical point of view, vibration has been shown to be analogous to thermal activation, and phase transitions between solid, liquid, and gas granular phases have been reported. The nature of this transition, taking into account dissipation, remains a subject of active debate [32].

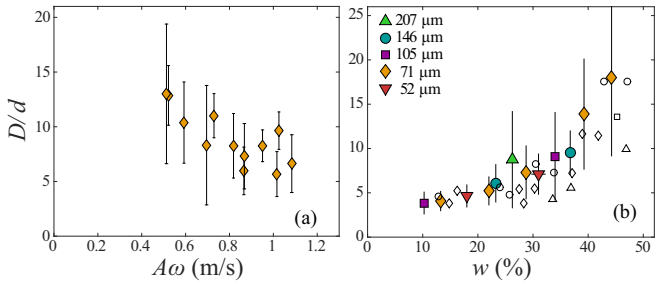

FIG. 4. (a) Agglomerate size normalized by the grain diameter, as a function of the vibration characteristic velocity $A\omega$. Here, $d = 71$ μm and $w = 30\%$. (b) Normalized agglomerate size as a function of the water content, for various grain diameters. Here, $A\omega = 0.9$ m/s, except for the open symbols that are high-shear granulation agglomerate sizes extracted from Ref. [2] with $d \approx 10$ μm and $\phi \approx 0.6$.

Working at a high water content and large acceleration ($A\omega^2/g \gg 1$), we observe that the system is not only fluidized but also forms spontaneously some nuclei or agglomerates. After mixing, the wet granular material is placed in one pile inside a hermetic box. It is then vibrated vertically with an amplitude A varying between 7 and 15 mm and a pulsation ω between 125 and 260 rad/s for typically 15 min. It breaks the pile into smaller pieces which form a granular gas of agglomerates: At the end of the experiment, we obtain bead clusters with an equilibrium size which does not depend on the size of the box or the quantity of grains. The same value is also obtained if the experiment is started with agglomerates smaller than their final size, showing that it is indeed the result of combined aggregation and fragmentation. The size of the agglomerates is then measured by taking a picture with a macroscope, as illustrated in Fig. 3(b): Fitting each agglomerate by an ellipse, we extract its geometrical diameter D°. Figure 3(c) presents the distribution of D° for various grain sizes and water content (about 1500 agglomerates in total), normalized by the mean value of each sample noted D. It is a relevant parameter to characterize these distributions since they are all similar despite variations in the experimental parameters. A Gaussian fit is plotted in Fig. 3(c) in order to highlight the slight asymmetry in these size distributions, which could be explained by a balance population model with adequate fitting parameters [33], but it exceeds the scope of our work. We now focus on the mean value of the agglomerate size D.

B. Results

We first investigate the effect of agitation, by studying the variations of D with both A and ω. Figure 4(a) shows that D decreases slightly with the characteristic vibration velocity: When $A\omega$ increases, more energy is available for fragmentation. But the main factor that prescribes the size of the aggregates is the liquid content. Figure 4(b) shows that the mean aggregate diameter D increases with the water content w. A comparison of these results with Fig. 2 shows a clear correlation of the agglomerate size with the cohesive strength: The more cohesive the agglomerate, the larger it is. Finally, for various bead sizes (tuned by a factor 4), D/d collapses on a single curve [Fig. 4(b)], stating that the number of grains in an agglomerate does not depend on the bead size, while the cohesive strength does (Fig. 2). For comparison, we also display data from high-shear granulation systems at a similar impeller rotation speed (close to 1 m/s with a typical size of the impeller of 10 cm and a typical particle size 10 μm) [2]. The agglomerates obtained with our simplified protocol are similar in size, although the details of the process are different. Moreover, it is worth mentioning that the effects of the typical velocity on the final size are also similar in industrial processes [1], suggesting that our setup is a promising model system to understand high-shear granulation.

C. Discussion

This result, showing that $D \propto d$, is quite unexpected. Indeed, a naive balance of the cohesive strength on the agglomerate surface (scaling as σD^2) with inertia (scaling as $\rho D^3 A\omega^2$) would result in $D \propto \sigma$, and since $\sigma \sim \gamma/d$, we deduce finally that $D \propto 1/d$, which is the inverse of the experimental result. If we consider dissipation due to the rupture energy of D^2/d^2 capillary bridges [17] and we balance it with the kinetic energy of the agglomerates, one recovers that $D \sim d^0$, also not satisfying our experimental results. The observed scaling law then gives us a strong constraint to model the granulation mechanism: For now, none of the physical models we tested accurately describes the nondependency of the aggregate number of grains with the bead size, in contrast to its key role in 2D viscous granulation processes, for example [34]. Some attempts taking into account the bistability of the agglomerate transiting under vibration from pendular to capillary states [35] could explain some of the observed results, but not convincingly. Moreover, the dynamics of impact and deformation of the wet granular material should be crucial in the aggregation process [2,27].

IV. CONCLUSION

To conclude, we show that the static cohesion of wet granular media saturates in a range of liquid fraction but then increases again at a high liquid content due to a saturation of the pressure in the liquid medium. Moreover, we show in a controlled dynamical experiment that high-shear granulation is a complex process where the number of granules per bead remains constant under given conditions. This experiment, showing self-similar agglomeration, opens the way to more controlled wet high-shear granulation processes as well as a deeper understanding of the interaction mechanisms in vibrated granular media.

ACKNOWLEDGMENT

The authors would like to thank Lyderic Bocquet and Nassira Benameur from Saint-Gobain Recherche for many scientific discussions, and an anonymous referee for suggestions concerning the modeling of the first part of the manuscript.

[1] B. J. Ennis, Agglomeration and size enlargement - Session summary paper, Powder Technol. **88**, 203 (1996).
[2] H. G. Kristensen, Particle agglomeration in high shear mixers, Powder Technol. **88**, 197 (1996).
[3] Agglomerate, in *Encyclopedia Britannica*, edited by H. Chisholm (Cambridge University Press, Cambridge, UK, 1911), Vol. 1, pp. 375–375.
[4] V. Mannings, Planet formation: Grainy pictures of new worlds, Nature (London) **393**, 117 (1998).
[5] J. B. Gurdon, A community effect in animal development, Nature (London) **336**, 772 (1988).
[6] T. C. Halsey and A. J. Levine, How Sandcastles Fall, Phys. Rev. Lett. **80**, 3141 (1998).
[7] D. J. Hornbaker, R. Albert, I. Albert, A.-L. Barabási, and P. Schiffer, What keeps sandcastles standing? Nature (London) **387**, 765 (1997).
[8] O. Pitois, P. Moucheront, and X. Chateau, Rupture energy of a pendular liquid bridge, Eur. Phys. J. B **23**, 79 (2001).
[9] L. Bocquet, E. Charlaix, and F. Restagno, Physics of humid granular media, C. R. Phys. **3**, 207 (2002).
[10] M. Pakpour, M. Habibi, P. Møller, and D. Bonn, How to construct the perfect sandcastle, Sci. Rep. **2**, 549 (2012).
[11] V. Richefeu, F. Radjaı, and M. S. El Youssoufi, Stress transmission in wet granular materials, Eur. Phys. J. E **21**, 359 (2007).

[12] M. Scheel, R. Seemann, M. Brinkmann, M. Di Michiel, A. Sheppard, B. Breidenbach, and S. Herminghaus, Morphological clues to wet granular pile stability, Nat. Mater. **7**, 189 (2008).
[13] J.-Y. Delenne, V. Richefeu, and F. Radjai, Liquid clustering and capillary pressure in granular media, J. Fluid Mech. **762**, 1 (2015).
[14] X. Chateau, P. Moucheront, and O. Pitois, Micromechanics of unsaturated granular media, J. Eng. Mech. **128**, 856 (2002).
[15] F. Restagno, L. Bocquet, and E. Charlaix, Where does a cohesive granular heap break? Eur. Phys. J. E **14**, 177 (2004).
[16] B. J. Ennis, Theory in granulation, in *Handbook of Pharmaceutical Granulation Technology*, 2nd ed. (Taylor & Francis, London, 2005), Vol. 2.
[17] S. Herminghaus, Dynamics of wet granular matter, Adv. Phys. **54**, 221 (2005).
[18] F. Soulié, M. S. El Youssoufi, F. Cherblanc, and C. Saix, Capillary cohesion and mechanical strength of polydisperse granular materials, Eur. Phys. J. E **21**, 349 (2006).
[19] C. Semprebon, M. Scheel, S. Herminghaus, R. Seemann, and M. Brinkmann, Liquid morphologies and capillary forces between three spherical beads, Phys. Rev. E **94**, 012907 (2016).
[20] H. Schubert, Capillary forces—modeling and application in particulate technology, Powder Technol. **37**, 105 (1984).
[21] W. Pietsch, E. Hoffman, and H. Rumpf, Tensile strength of moist agglomerates, Ind. Eng. Chem. Prod. Res. Dev. **8**, 58 (1969).
[22] T. Ruiz, M. Delalonde, B. Bataille, G. Baylac, and C. Dupuy de Crescenzo, Texturing unsaturated granular media submitted to compaction and kneading processes, Powder Technol. **154**, 43 (2005).
[23] P. Pierrat and H. S. Carram, Tensile strength of wet granular materials, Powder Technol. **91**, 83 (1997).
[24] E. Koos and N. Willenbacher, Capillary forces in suspension rheology, Science **331**, 897 (2011).
[25] M. Scheel, R. Seemann, M. Brinkmann, M. Di Michiel, A. Sheppard, and S. Herminghaus, Liquid distribution and cohesion in wet granular assemblies beyond the capillary bridge regime, J. Phys.: Condens. Matter **20**, 494236 (2008).
[26] N. Lu, B. Wu, and C. P. Tan, Tensile strength characteristics of unsaturated sands, J. Geotech. Geoenviron. Eng. **133**, 144 (2007).
[27] J. Fu, G. K. Reynolds, M. J. Adams, J. Michael, M. J. Hounslow, and A. D Salman, An experimental study of the impact breakage of wet granules, Chem. Eng. Sci. **60**, 4005 (2005).
[28] J. E. Fiscina, G. Lumay, F. Ludewig, and N. Vandewalle, Compaction Dynamics of Wet Granular Assemblies, Phys. Rev. Lett. **105**, 048001 (2010).
[29] J. Li, Y. Cao, C. Xia, B. Kou, X. Xiao, K. Fezzaa, and Y. Wang, Similarity of wet granular packing to gels, Nat. Commun. **5**, 5014 (2014).
[30] M. Argentina, M. G. Clerc, and R. Soto, van der Waals-Like Transition in Fluidized Granular Matter, Phys. Rev. Lett. **89**, 044301 (2002).
[31] J. P. D. Clewett, K. Roeller, R. M. Bowley, S. Herminghaus, and M. R. Swift, Emergent Surface Tension in Vibrated, Noncohesive Granular Media, Phys. Rev. Lett. **109**, 228002 (2012).
[32] J. P. D. Clewett, J. Wade, R. M. Bowley, S. Herminghaus, M. R. Swift, and M. G. Mazza, The minimization of mechanical work in vibrated granular matter, Sci. Rep. **6**, 28726 (2016).
[33] C. F. W Sanders, A. W. Willemse, A. D Salman, and M. J. Hounslow, Development of a predictive high-shear granulation model, Powder Technol. **138**, 18 (2003).
[34] K. Huang, M. Brinkmann, and S. Herminghaus, Wet granular rafts: Aggregation in two dimensions under shear flow, Soft Matter **8**, 11939 (2012).
[35] M. E. Cates and M. Wyart, Granulation and bistability in non-Brownian suspensions, Rheol. Acta **53**, 755 (2014).